Supplementary Material

Deep sea biofilms, historic shipwreck preservation and the *Deepwater Horizon* spill

Rachel L. Mugge[1], Melissa L. Brock[1], Jennifer L. Salerno[2], Melanie Damour[3], Robert A. Church[4], Jason Lee[5], and Leila J. Hamdan*[1]

*** Correspondence:** Leila J. Hamdan, leila.hamdan@usm.edu

1. Supplementary Data

Detailed Site Information

Anona is a steel-hulled, steam-propelled former pleasure yacht built in 1904 and sunk in 1944. The wreck lies in approximately 1,200 m (3,900 ft.) of water about 55 km (34 mi.) northeast of the DWH spill origin. The site was discovered during a 1995 oil and gas survey but was not investigated until 2002 when a remotely operated vehicle (ROV) inspection was conducted. The hull measures approximately 43 m (141 ft.) long by 5 m (16 ft.) wide with a maximum of 2.2 m (7.2 ft.) of relief above the seafloor amidships (Warren et al. 2016:64).

The Viosca Knoll Wreck is a 19th century copper-sheathed, wooden-hulled sailing vessel lying in approximately 600 m (1,900 ft.) of water more than 78 km (48 mi.) to the northeast of the DWH spill origin. The wreck was discovered in 2003 during an oil and gas pipeline survey and found to have been impacted during the installation of a nearby oil and gas platform. Archaeologists have investigated the site several times since 2006 using ROVs and autonomous underwater vehicles (AUVs). The hull measures between 37 and 43 m (121–141 ft.) long by 8 m (26 ft.) wide with up to 3 m (10 ft.) of relief above the seafloor (Warren et al. 2016:63).

The Mica Wreck is another 19th century copper-sheathed, wooden-hulled sailing vessel. The wreck lies in approximately 800 m (2,600 ft.) of water less than 25 km (15 mi.) to the northwest of the DWH spill origin. This previously unknown site was discovered in 2001 during a post-installation pipeline inspection, which found that the pipeline had been inadvertently laid perpendicularly across the hull (port and starboard sides) causing irreparable damage. The site was the subject of a data recovery and investigation by archaeologists in 2003. The hull measures approximately 20 m (65 ft.) long by 6 m (20 ft.) wide with up to 3 m (10 ft.) of relief above the seafloor (Warren et al. 2016:63).

U-166 is the remains of a Type IXC German U-boat sunk by U.S. Navy patrol craft *PC-566* in 1942, the only U-boat sunk in the Gulf during World War II. The hull exploded and broke apart into two sections after being struck by depth charges. The bow and stern sections and an extensive debris field between them cover an area of seafloor over approximately 7.52 hectares (18 acres). The sections lie in approximately 1,500 m (4,900 ft.) of water only 8 kilometers (4.9 miles) to the southwest of the DWH spill origin. The site was first discovered during a 1986 oil and gas survey but was not identified as *U-166* until a subsequent AUV survey in 2001 and a follow-up ROV investigation by archaeologists. The bow section measures approximately 20 m (65 ft.) long by 6.7 m (22 ft.) wide with less than 1 m (3.3 ft.) of relief above the seafloor. The stern section containing the conning tower measures roughly 55 m (180 ft.) long by 6.7 m (22 ft.) wide with less than 1 m (3.3 ft.) of relief except for the conning tower which extends 5 m (16 ft.) above the seafloor (Warren et al. 2016:62).

The Ewing Bank Wreck is a 19th century copper-sheathed, wooden-hulled sailing vessel lying in more than 600 m (1,970 ft.) of water over 190 km (120 mi.) to the west of the DWH spill origin. The shipwreck was discovered during an AUV survey in 2006 and was first investigated by archaeologists using an ROV in 2008. The hull measures approximately 36.5 m (110 ft.) long by 10 m (33 ft.) wide with 3 m (10 ft.) of relief above the seafloor (Warren et al. 2016:65).

Halo is an American steel-hulled oil tanker built in 1920 and sunk in 1942 by the German U-boat *U-506*. The wreck lies in approximately 140 m (460 ft.) of water more than 165 km (100 mi.) west of the DWH spill origin. The site was discovered during a pipeline survey in 2000 and first investigated by archaeologists using an ROV in 2004. The hull measures 133 m (436 ft.) long by 17 m (55 ft.) wide with a maximum of 16.5 m (54 ft.) of relief above the seafloor (Warren et al. 2016:64–65).

Refs Cited:

Damour, Melanie, Robert Church, Daniel Warren, Christopher Horrell, and Leila J. Hamdan. 2016. "Gulf of Mexico Shipwreck Corrosion, Hydrocarbon Exposure, Microbiology, and Archaeology (GOM-SCHEMA) Project: Studying the Effects of a Major Oil Spill on Submerged Cultural Resources." In Marco Meniketti (ed.) ACUA Underwater Archaeology Proceedings of the 2015 Annual Meeting of the Society for Historical Archaeology, Seattle, WA, pgs. 49–59.

Warren, Daniel J., Robert A. Church, and Robert F. Westrick. 2016. "Oil and Shipwrecks: An Overview of the Sites Selected for the Gulf of Mexico Shipwreck Corrosion, Hydrocarbon Exposure, Microbiology, and Archaeology (GOM-SCHEMA) Project." In Marco Meniketti (ed.) ACUA Underwater Archaeology Proceedings of the 2015 Annual Meeting of the Society for Historical Archaeology, Seattle, WA, pgs. 61–68.

2. Supplementary Tables

Supplementary Table Legends

Table S1. Permutational Analysis of Variance (PERMANOVA). The analysis was conducted on biofilm samples to determine differences based on depth, impact, and hull type. Depth was used as a covariate, and factors of impact and hull type were fit to the model, including contrasts between different levels of impact. PERMANOVA was run using Type I (sequential) sum of squares, fixed effects sum to zero, permutation of residuals under a reduced model, and 9999 permutations.

Table S2. SourceTracker results of the proportion of the top 10 OTUs sourced from sediments in all biofilm samples (top) and biofilms from individual sites (bottom).

Table S3. SourceTracker analysis of core microbiome OTUs in biofilms and their predicted source proportion from sediment.

Table S4. Top 10 Differentially Abundant Genes (DAGs) from analysis in EdgeR. Read counts of genes were converted to counts per million (CPM) to correct for differences in library size. Differential abundance analysis was run on reference sites against impacted sites. A negative log fold change value represents a higher abundance of the gene at reference sites while a positive value represents higher gene abundance at impacted sites.

Supplementary Tables

Table S1. Permutational Analysis of Variance (PERMANOVA). The analysis was conducted on biofilm samples to determine differences based on depth, impact, and hull type. Depth was used as a covariate, and factors of impact and hull type were fit to the model, including contrasts between different levels of impact. PERMANOVA was run using Type I (sequential) sum of squares, fixed effects sum to zero, permutation of residuals under a reduced model, and 9999 permutations.

Source	df	SS	MS	Pseudo-F	P (perm)	Unique perms	P (MC)
Depth	1	5388.5	5388.5	10.258	0.0001	9897	0.0001
Impact	2	2876	1438	2.7375	0.0001	9820	0.0001
Reference vs Moderate	1	2958.3	2958.3	5.1819	0.0002	9876	0.0003
Reference vs Heavy	1	1356.4	1356.4	2.4376	0.0001	9866	0.0053
Moderate vs Heavy	1	1461.8	1461.8	3.359	0.0001	9887	0.002
Hull Type	1	3342.3	3342.3	6.3627	0.0001	9889	0.0001

Table S2. SourceTracker results of the proportion of the top 10 OTUs sourced from sediments in all biofilm samples (top) and biofilms from individual sites (bottom).

OTU ID	Taxonomy	Proportion
Otu2	Gammaproteobacteria; Alteromonadales; Colwelliaceae	4.34%
Otu11	Alphaproteobacteria; Rhodobacterales; Rhodobacteraceae	1.27%
Otu13	Alphaproteobacteria; Rhodobacterales; Rhodobacteraceae	1.06%
Otu10	Alphaproteobacteria; Rhodobacterales; Rhodobacteraceae	0.75%
Otu9	Alphaproteobacteria; Rhodobacterales; Rhodobacteraceae; Octadecabacter	0.75%
Otu12	Alphaproteobacteria; Rhodobacterales; Rhodobacteraceae	0.63%
Otu7	Zetaproteobacteria; Mariprofundales; Mariprofundaceae; Mariprofundus	0.52%
Otu35	Alphaproteobacteria; Rhodobacterales; Rhodobacteraceae; Phaeobacter	0.45%
Otu23	Gammaproteobacteria; Alteromonadales; Alteromonadaceae; HB2-32-21	0.39%
Otu47	Flavobacteriia; Flavobacteriales; Flavobacteriaceae	0.32%

Site Name	OTU ID	Taxonomy	Proportion
Anona	Otu2	Gammaproteobacteria; Alteromonadales; Colwelliaceae	5.64%
	Otu13	Alphaproteobacteria; Rhodobacterales; Rhodobacteraceae; Octadecabacter	1.95%
	Otu12	Alphaproteobacteria; Rhodobacterales; Rhodobacteraceae	1.71%
	Otu10	Alphaproteobacteria; Rhodobacterales; Rhodobacteraceae; Octadecabacter; antarcticus	1.60%
	Otu7	Zetaproteobacteria; Mariprofundales; Mariprofundaceae; Mariprofundus	1.48%
	Otu47	Flavobacteriia; Flavobacteriales; Flavobacteriaceae	1.02%
	Otu23	Gammaproteobacteria; Alteromonadales; Alteromonadaceae; HB2-32-21	0.92%
	Otu25	Gammaproteobacteria; Alteromonadales; Colwelliaceae	0.89%
	Otu11	Alphaproteobacteria; Rhodobacterales; Rhodobacteraceae	0.84%
	Otu9	Alphaproteobacteria; Rhodobacterales; Rhodobacteraceae; Octadecabacter	0.77%
Ewing Bank	Otu2	Gammaproteobacteria; Alteromonadales; Colwelliaceae	7.16%
	Otu9	Alphaproteobacteria; Rhodobacterales; Rhodobacteraceae; Octadecabacter	1.87%
	Otu11	Alphaproteobacteria; Rhodobacterales; Rhodobacteraceae;	1.33%
	Otu35	Alphaproteobacteria; Rhodobacterales; Rhodobacteraceae; Phaeobacter	0.45%
	Otu13	Alphaproteobacteria; Rhodobacterales; Rhodobacteraceae; Octadecabacter	0.38%
	Otu10	Alphaproteobacteria; Rhodobacterales; Rhodobacteraceae; Octadecabacter; antarcticus	0.23%
	Otu7	Zetaproteobacteria; Mariprofundales; Mariprofundaceae; Mariprofundus	0.17%
	Otu143	Alphaproteobacteria; Rhizobiales; Phyllobacteriaceae	0.10%
	Otu23	Gammaproteobacteria; Alteromonadales; Alteromonadaceae; HB2-32-21	0.09%
	Otu83	Flavobacteriia; Flavobacteriales; Flavobacteriaceae	0.07%
Halo	Otu47	Flavobacteriia; Flavobacteriales; Flavobacteriaceae	0.51%
	Otu132	Deltaproteobacteria; Desulfuromonadales; Desulfuromonadaceae	0.20%
	Otu213	Cytophagia; Cytophagales; Flammeovirgaceae	0.12%
	Otu184	Alphaproteobacteria; Rhodobacterales; Rhodobacteraceae	0.10%
	Otu35	Alphaproteobacteria; Rhodobacterales; Rhodobacteraceae; Phaeobacter	0.07%
	Otu33	Gammaproteobacteria; Thiotrichales; Piscirickettsiaceae	0.06%
	Otu12	Alphaproteobacteria; Rhodobacterales; Rhodobacteraceae	0.06%
	Otu10	Alphaproteobacteria; Rhodobacterales; Rhodobacteraceae; Octadecabacter; antarcticus	0.05%
	Otu11	Alphaproteobacteria; Rhodobacterales; Rhodobacteraceae	0.05%
	Otu8211	Alphaproteobacteria; Rhodobacterales; Rhodobacteraceae	0.04%
Mica	Otu2	Gammaproteobacteria; Alteromonadales; Colwelliaceae	2.58%
	Otu13	Alphaproteobacteria; Rhodobacterales; Rhodobacteraceae; Octadecabacter	1.33%
	Otu11	Alphaproteobacteria; Rhodobacterales; Rhodobacteraceae	1.17%
	Otu12	Alphaproteobacteria; Rhodobacterales; Rhodobacteraceae	1.12%
	Otu9	Alphaproteobacteria; Rhodobacterales; Rhodobacteraceae; Octadecabacter	0.91%
	Otu35	Alphaproteobacteria; Rhodobacterales; Rhodobacteraceae; Phaeobacter	0.66%
	Otu37	Gammaproteobacteria; Thiotrichales; Thiotrichaceae	0.53%
	Otu10	Alphaproteobacteria; Rhodobacterales; Rhodobacteraceae; Octadecabacter; antarcticus	0.30%
	Otu23	Gammaproteobacteria; Alteromonadales; Alteromonadaceae; HB2-32-21	0.22%
	Otu17	Alphaproteobacteria; Rhodobacterales; Rhodobacteraceae	0.21%
U-166	Otu2	Gammaproteobacteria; Alteromonadales; Colwelliaceae	6.54%
	Otu11	Alphaproteobacteria; Rhodobacterales; Rhodobacteraceae	2.88%
	Otu13	Alphaproteobacteria; Rhodobacterales; Rhodobacteraceae; Octadecabacter	1.79%
	Otu10	Alphaproteobacteria; Rhodobacterales; Rhodobacteraceae; Octadecabacter; antarcticus	1.73%
	Otu7	Zetaproteobacteria; Mariprofundales; Mariprofundaceae; Mariprofundus	1.01%
	Otu23	Gammaproteobacteria; Alteromonadales; Alteromonadaceae; HB2-32-21	0.80%
	Otu279	Alphaproteobacteria; Rhodobacterales; Rhodobacteraceae	0.73%
	Otu35	Alphaproteobacteria; Rhodobacterales; Rhodobacteraceae; Phaeobacter	0.38%
	Otu12	Alphaproteobacteria; Rhodobacterales; Rhodobacteraceae	0.36%
	Otu17	Alphaproteobacteria; Rhodobacterales; Rhodobacteraceae	0.30%

Table S3. SourceTracker analysis of core microbiome OTUs in biofilms and their predicted source proportion from sediment.

OTU ID	Taxonomy	Proportion	Functional roles in published literature
Otu10	Alphaproteobacteria; Rhodobacterales; Rhodobacteraceae; Octadecabacter; antarcticus	0.8%	biofilm former
Otu35	Alphaproteobacteria; Rhodobacterales; Rhodobacteraceae; Phaeobacter	0.5%	biofilm former
Otu11	Alphaproteobacteria; Rhodobacterales; Rhodobacteraceae	1.3%	biofilm former
Otu9	Alphaproteobacteria; Rhodobacterales; Rhodobacteraceae; Octadecabacter	0.8%	biofilm former
Otu7	Zetaproteobacteria; Mariprofundales; Mariprofundaceae; Mariprofundus	0.5%	iron oxidizer
Otu13	Alphaproteobacteria; Rhodobacterales; Rhodobacteraceae; Octadecabacter	2.1%	biofilm former
Otu23	Gammaproteobacteria; Alteromonadales; Alteromonadaceae; HB2-32-21	0.8%	unknown
Otu1	Zetaproteobacteria; Mariprofundales; Mariprofundaceae; Mariprofundus	0.0%	iron oxidizer
Otu87	Zetaproteobacteria; Mariprofundales; Mariprofundaceae; Mariprofundus	0.0%	iron oxidizer
Otu27	Gammaproteobacteria; Chromatiales	0.0%	sulfur reducer
Otu16	Zetaproteobacteria; Mariprofundales; Mariprofundaceae; Mariprofundus	0.0%	iron oxidizer

Table S4. Top 10 Differentially Abundant Genes (DAGs) from analysis in EdgeR. Read counts of genes were converted to counts per million (CPM) to correct for differences in library size. Differential abundance analysis was run on reference sites against impacted sites. A negative log fold change value represents a higher abundance of the gene at reference sites while a positive value represents higher gene abundance at impacted sites.

Gene	logFC	logCPM	PValue	FDR
Two-component response regulator CreC	-6.02	7.05	0.00	0.01
Nitrate ABC transporter, nitrate-binding protein	-1.87	9.19	0.00	0.08
Potassium channel protein 1 (MjK1)	5.45	3.82	0.00	0.08
Nitrate ABC transporter, permease protein	-1.99	8.45	0.00	0.24
StbE replicon stabilization toxin	3.77	4.71	0.00	0.24
Sorbitol-6-phosphate 2-dehydrogenase (EC 1.1.1.140)	4.10	5.45	0.00	0.24
Positive regulator of L-idonate catabolism	4.80	3.28	0.00	0.26
Indolepyruvate oxidoreductase subunit IorA (EC 1.2.7.8)	-2.71	6.77	0.00	0.26
Dihydroneopterin triphosphate pyrophosphohydolase type 2	6.66	3.07	0.00	0.26
Indolepyruvate oxidoreductase subunit IorB (EC 1.2.7.8)	-3.24	4.20	0.00	0.31

3. Supplementary Figures

Supplementary Figure Legends

Figure S1. Class level bacterial community composition (16S rRNA) in surface (0–4 cm below the seafloor) sediment samples collected within 2 m of historic shipwrecks.

Figure S2. Class level bacterial community composition (16S rRNA) in water samples collected ~10m above historic shipwrecks.

Figure S3. SourceTracker prediction of potential microbiome sources to biofilm samples. Results are averages for replicate samples.

Figure S4. Bubble plot of abundances of gene families obtained from the MEGAN software using the SEED database for functional classification. Size of bubble corresponds to counts of gene in a gene family.

Figure S5. Metal loss (g) on carbon steel disks over the duration of the experiment. Error bars are standard error.

Supplementary Figures

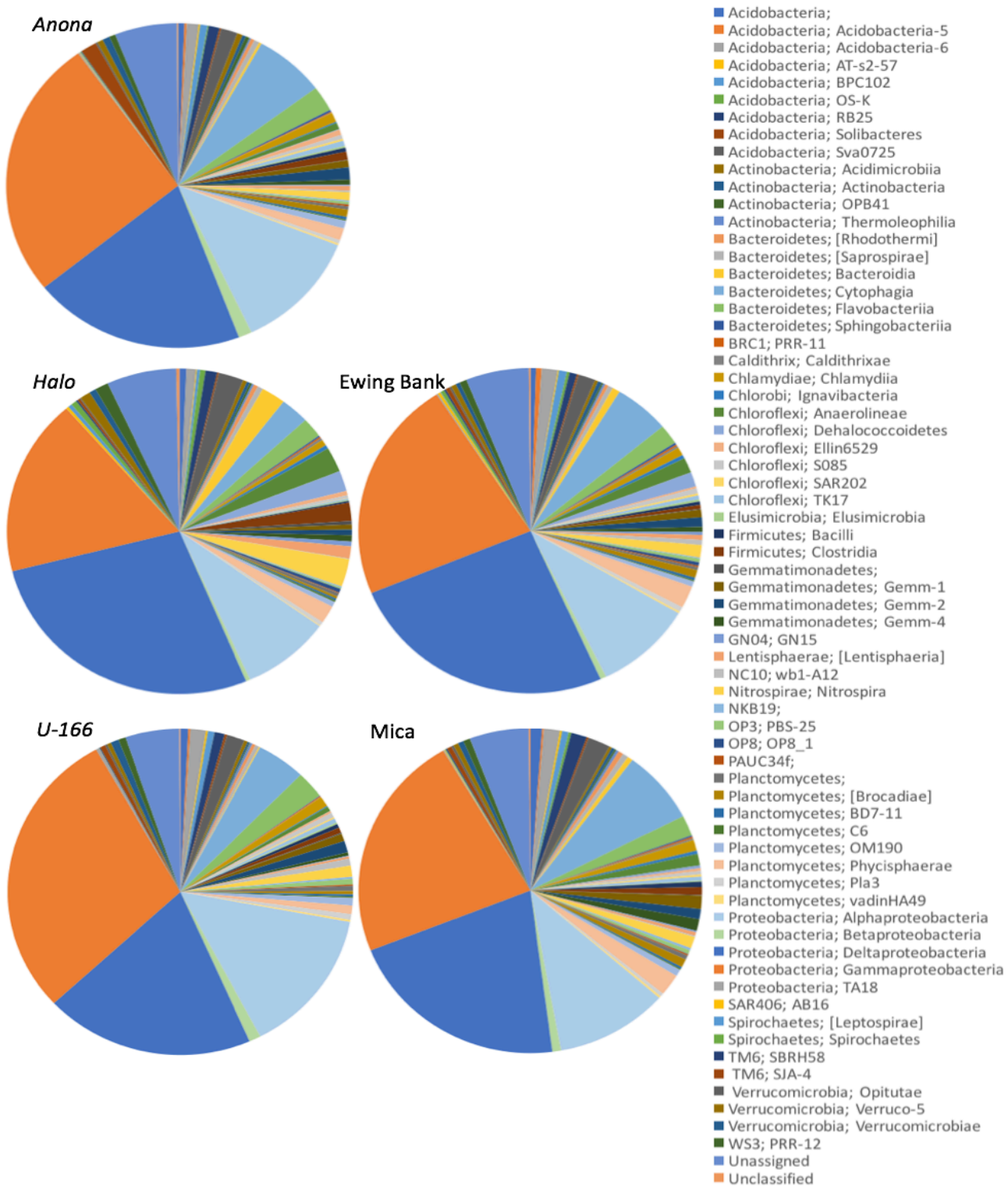

Supplementary Figure 1. Class level bacterial community composition (16S-rRNA) in surface (0-4 cm below the seafloor) sediment samples collected within 2 m of historic shipwrecks.

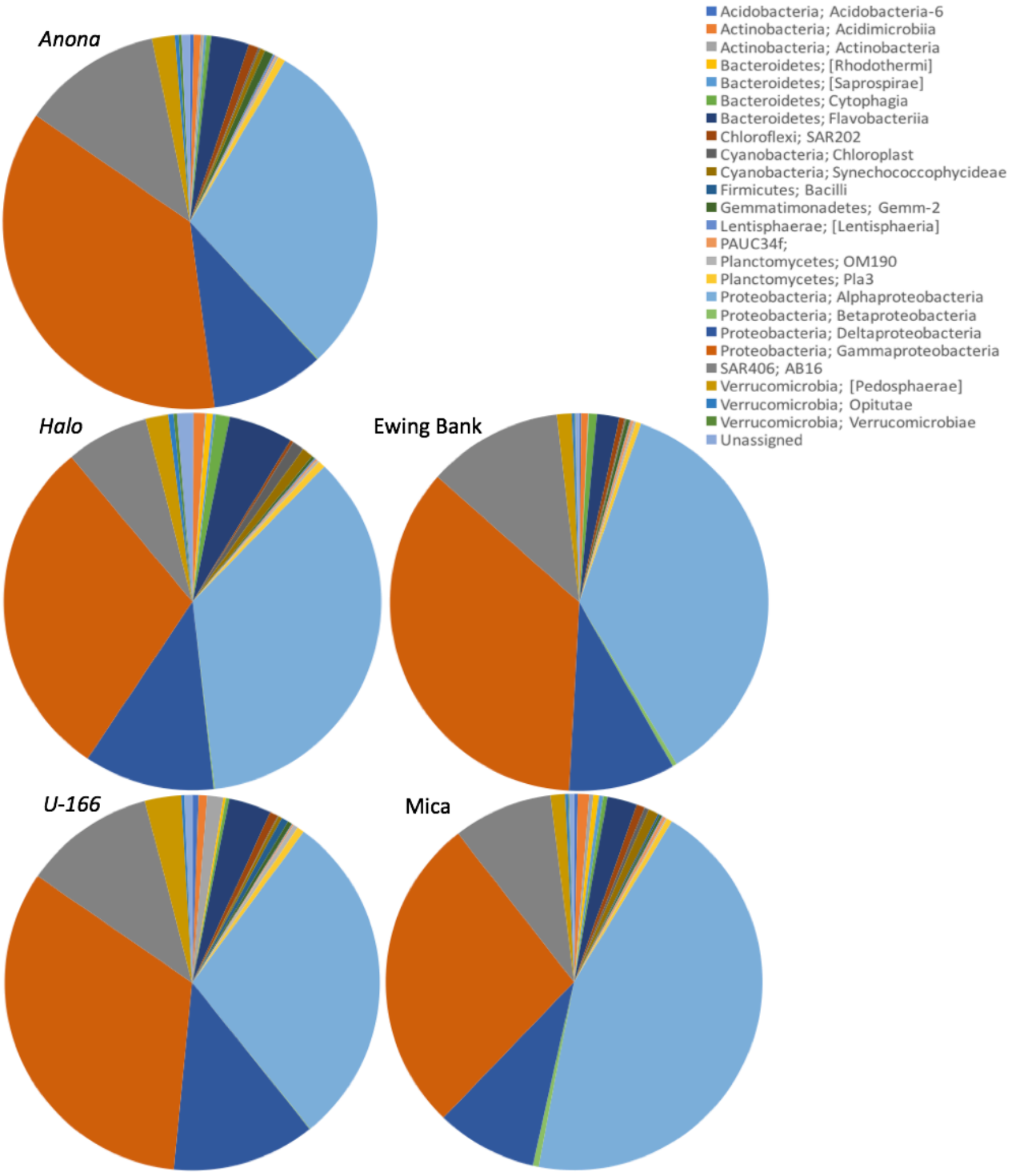

Supplementary Figure 2. Class level bacterial community composition (16S-rRNA) in water samples collected ~10m above historic shipwrecks.

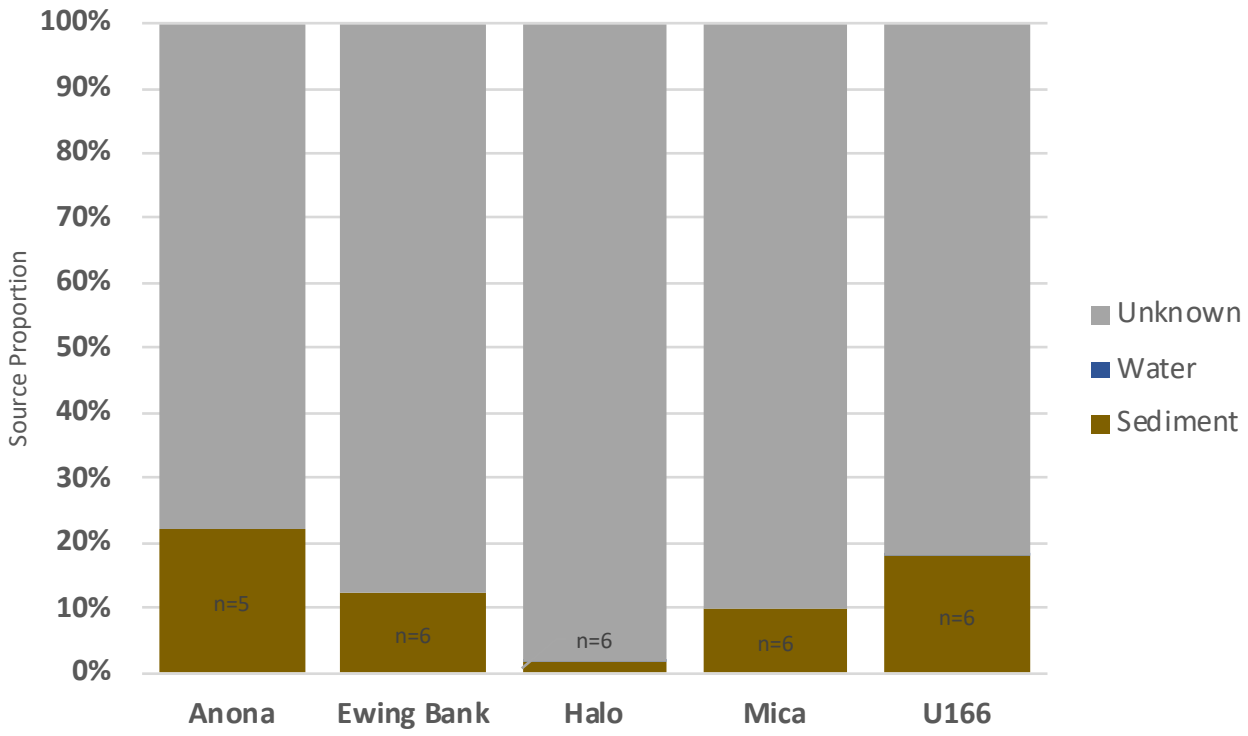

Supplementary Figure 3. SourceTracker prediction of potential microbiome sources to biofilm samples. Results are averages for replicate samples.

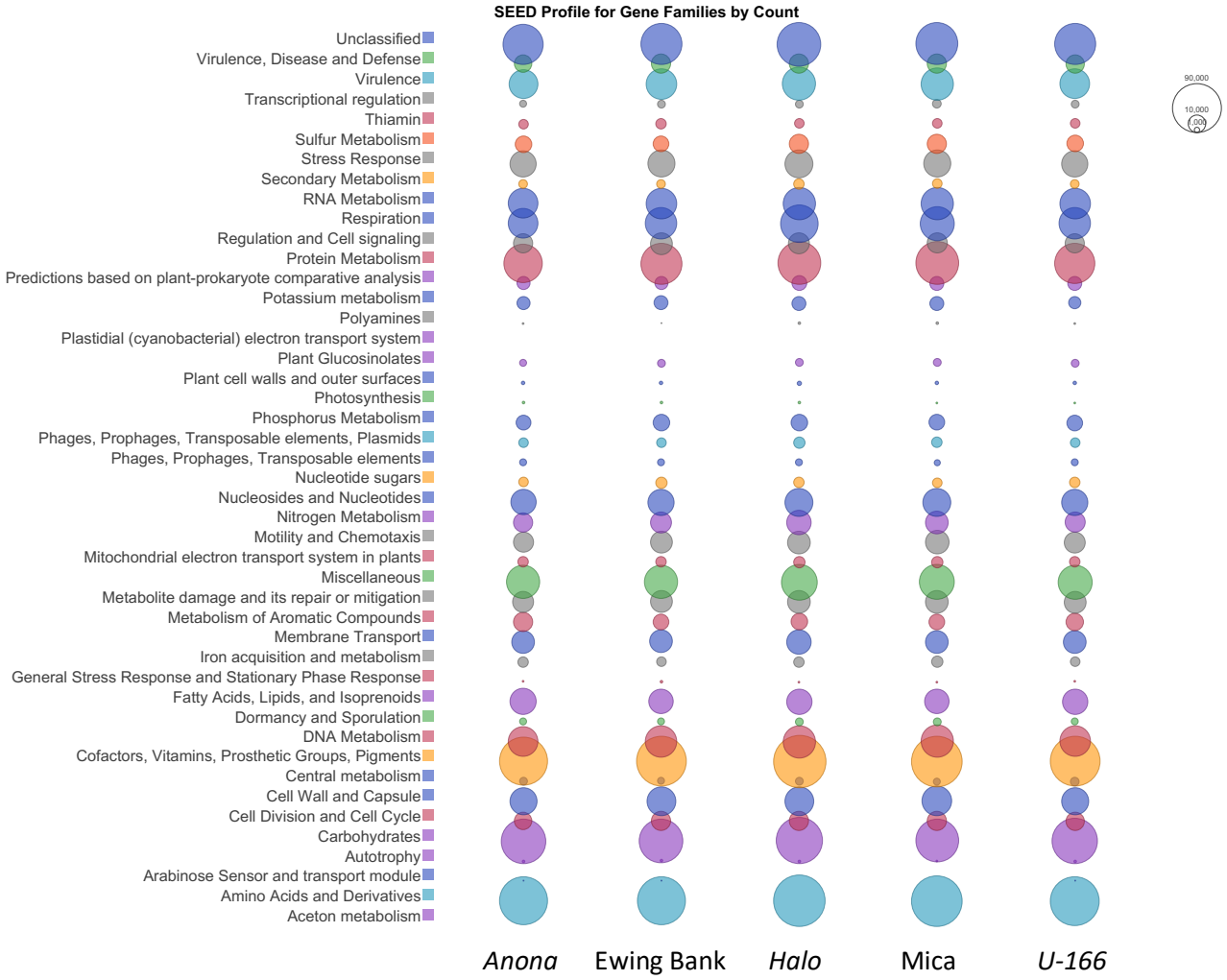

Supplementary Figure 4. Bubble plot of abundances of gene families obtained from the MEGAN software using the SEED database for functional classification. Size of bubble corresponds to counts of genes in a gene family.

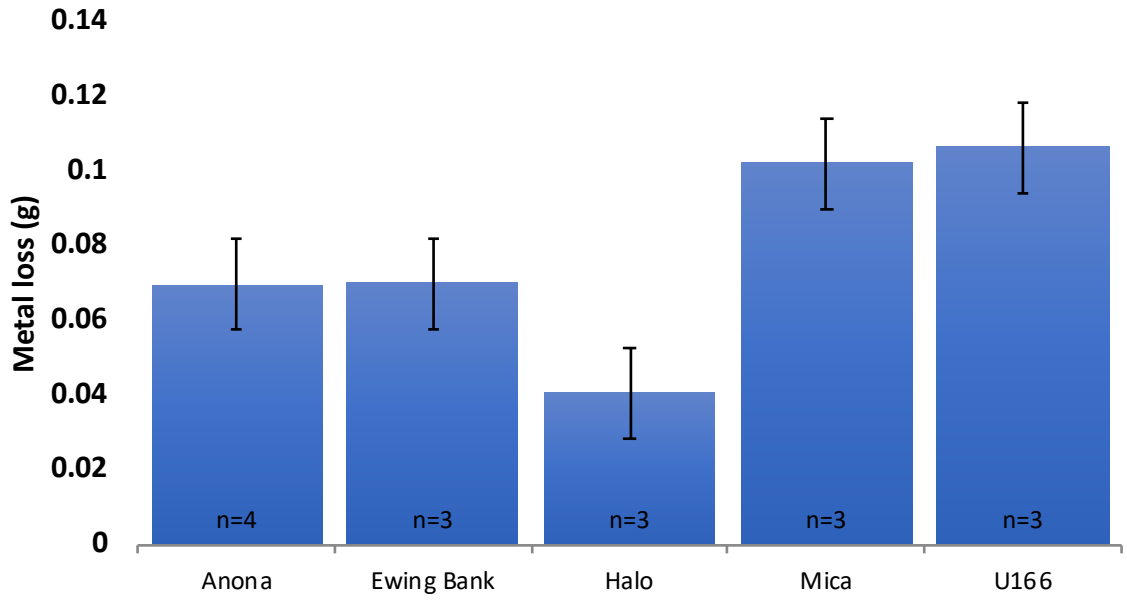

Supplementary Figure 5. Metal loss (g) on carbon steel disks over the duration of the experiment. Error bars are standard error.